A SIMPLIFIED METHOD FOR MEASUREMENT OF AIR FLOW RATES IN FLAT OVAL DUCTS

by

TERRENCE D. MAYHILL

B. S., Kansas State University, 1970

A THESIS

submitted in partial fulfillment of the

requirements for the degree

MASTER OF SCIENCE

Department of Mechanical Engineering

KANSAS STATE UNIVERSITY
Manhattan, Kansas

1971

Approved by:

Major Professor

PREFACE

My sincerest thanks to the following individuals in appreciation of their generous assistance:

Dr. P. L. Miller, my major advisor, whose reflections and advice have guided me throughout the undertaking of this thesis.

My advisory committee, Professors R. L. Gorton and C. L. Huang for their judgement and recommendations.

My wife, Sherry, for her endless patience, her day to day encouragements, her reflections upon the topic of this thesis, and her hours of assistance in its preparation.

United Sheet Metal Division, United McGill Corporation of Westerville, Ohio; SEMCO of Salisbury, Missouri; and Sheet Metal Products Company of El Paso, Texas, for their donations of the test materials used in this investigation.

National Science Foundation, for their financial assistance during my graduate studies.

TABLE OF CONTENTS

LIST OF TABLES

LIST OF FIGURES

Figure | Page

NOMENCLATURE

A	duct cross sectional area (ft^2)
A.R.	duct aspect ratio; (major axis/minor axis)
C_F	flow coefficient (mean duct velocity/duct centerline velocity)
D	duct dimension, diameter of semicircular end on duct (ft)
D_H	duct hydraulic diameter (4·duct area/duct perimeter) (ft)
h	velocity pressure (in. H_2O)
L	duct dimension, major axis (ft)
R	duct dimension, radius of semicircular end on duct (ft)
Re	Reynolds' number $\overline{V}D_H/\nu$
V	velocity (ft/min)
$\overline{V}$	mean duct velocity (ft/min)
$V_{℄}$	duct centerline velocity (ft/min)
Q	volumetric flow rate (ft^3/min)

Greek

ν	kinematic viscosity (ft^2/min)

CHAPTER I

INTRODUCTION

In recent years, the air handling industry has begun using a flat oval shaped duct designed for low headroom spaces and restricted ceiling plenum spaces. The flat oval duct shape consists of a rectangular cross section coupled with a semicircular section on each end of a rectangle (1)*. Figure 1 below illustrates the nomenclature used to describe the flat oval shape.

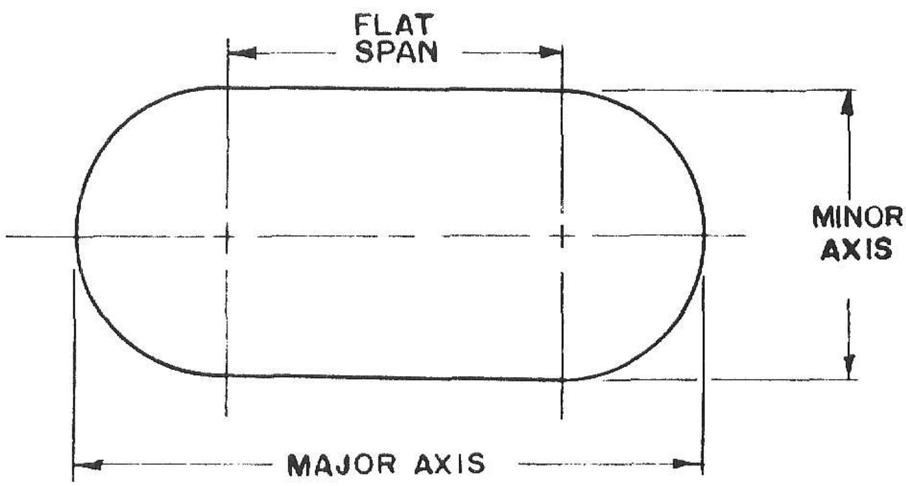

Figure 1. Nomenclature used to describe the flat oval shape.

The dimension of the cross section is given as minor axis versus major axis. The flat span is sometimes given as a fundamental dimension

*Numbers in parentheses designate References at the end of the thesis. (page 35) and is the distance between the centers of the semicircular ends. The aspect ratio of the flat oval shape is defined as the major axis divided by the minor axis. The distinct low profile of the flat oval ducts provides a comparatively large cross sectional area with a relatively small minor axis. The flat oval shape has considerably less flat surface than a comparable rectangular duct. This difference in relative flat surface areas has accoustical, structural, and installation significance (2).

Since these ducts are relatively new to the air handling industry, test data is somewhat scarce. At the present time there is no proven, practical method for the measurement of volumetric air flow rates in flat oval ducts. Channeling the air through a standard measuring section is the only proven method, but this is troublesome and expensive. The ideal situation would be to measure only one velocity, the centerline velocity, and multiply this velocity by a single known flow coefficient and the duct area to obtain the desired air flow rate. This flow coefficient is defined as the mean duct velocity divided by the centerline velocity. A proven method of traversing the flat oval ducts should also be available to provide a more precise procedure to obtain the duct mean velocity. Methods for traversing standard round and rectangular ducts are given in (3).

With the idea in mind that a method of traversing flat oval ducts and a flow coefficient for flat oval ducts would greatly simplify the measurement of flow in these duct systems, the objectives of this research were:

1. To develop a method of traversing flat oval ducts to obtain the mean velocity within the duct.

2. To develop a correlation between flow coefficient and some dimensionless parameter. This parameter, in conjunction with

> a single point velocity measurement at the duct centerline, would be used to determine the mean velocity within the duct.

Since these ducts are mainly utilized in heating, ventilating and air conditioning systems, fully developed flow is seldom obtained. Therefore, this investigation was done in the duct entrance region prior to fully developed flow. In order to correspond to the actual conditions of duct application, this investigation was done with isothermal air and turbulent flow.

CHAPTER II

EXPERIMENTAL PROGRAM

The following paragraphs describe the experimental equipment used, the test ducts used, and the procedures used in the experimental program.

Test Apparatus

A schematic diagram of the entire experimental assembly used in this investigation is shown in Fig. 2. It consists of a centrifugal blower, a plenum chamber, a measuring section using standard ASME long-radius nozzles, and the test section.

A ten horsepower direct current motor was used to drive the centrifugal blower. The d.c. motor was used to allow coarse adjustment in the air flow rate through the system. A slide damper on the blower inlet allowed fine adjustment. The motor and fan combination were capable of moving 2500 cfm of air through a 3.0 inches H_2O pressure drop. The fan was connected through a 12 inch round duct to a plenum chamber. The chamber measured 4'x4'x8'. Inside the plenum chamber were baffles and screens arranged to dampen fluctuations from the fan. The plenum chamber discharged to a 14" round duct. The measurement section consisted of a standard ASME long-radius nozzle with a honey-comb straightening vane placed 3 duct diameters down stream of the elbow and 6 duct diameters upstream of the flow nozzle in accord with ASME flow measurement recommendations (4). Two standard ASME long radius nozzles were used. Below 600 cfm

THIS BOOK CONTAINS NUMEROUS PAGES WITH DIAGRAMS THAT ARE CROOKED COMPARED TO THE REST OF THE INFORMATION ON THE PAGE.

THIS IS AS RECEIVED FROM CUSTOMER.

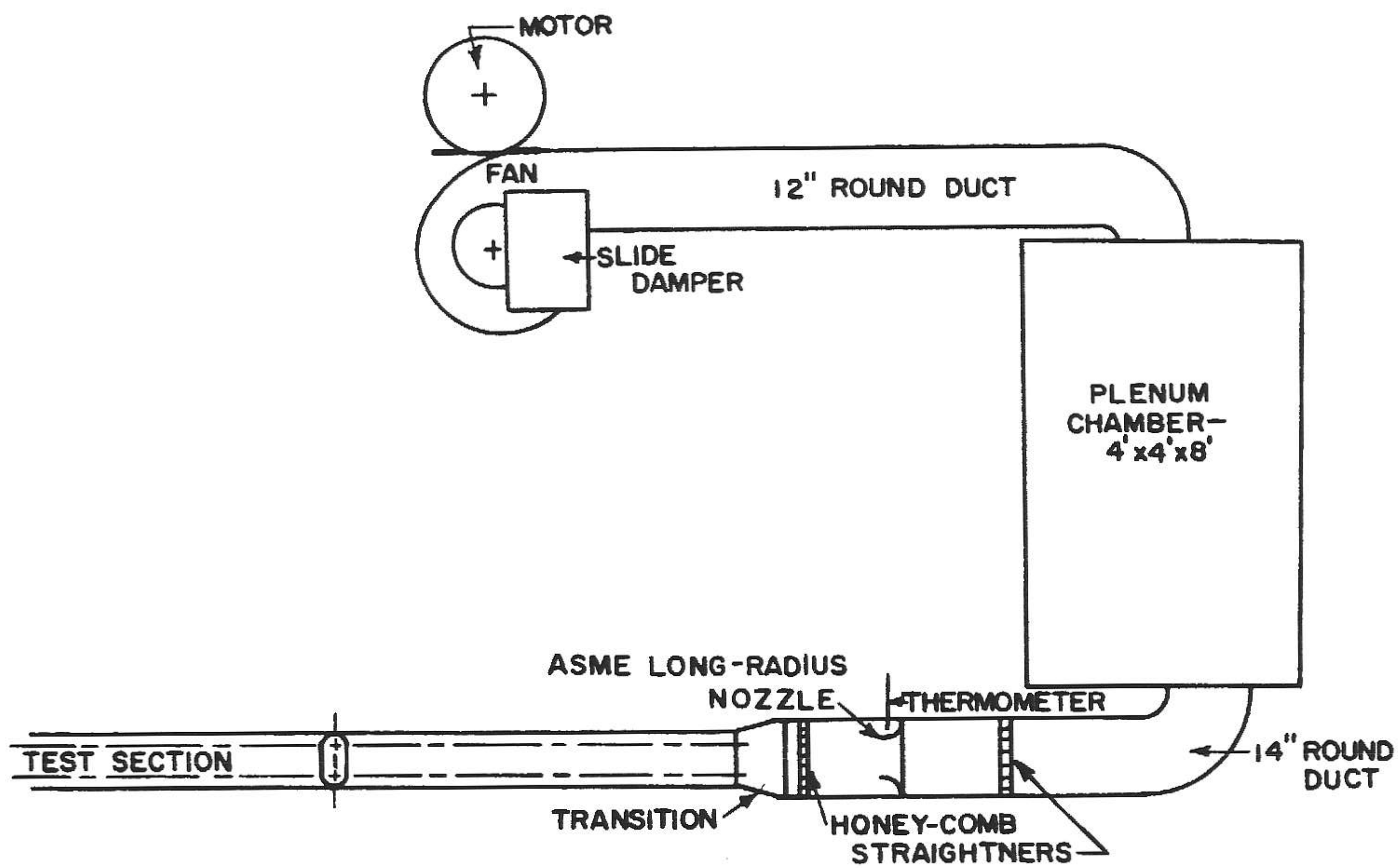

Figure 2. Schematic of Experimental Assembly.

THIS BOOK CONTAINS NUMEROUS PAGES WITH THE ORIGINAL PRINTING BEING SKEWED DIFFERENTLY FROM THE TOP OF THE PAGE TO THE BOTTOM.

THIS IS AS RECEIVED FROM THE CUSTOMER.

a 4" long-radius nozzle was used and above 600 cfm a 6" long-radius nozzle was used. Both nozzles were calibrated over their respective ranges of application. A second honey-comb was positioned 3 duct diameters downstream of the nozzle exit to insure a symmetric, flat profile at the entrance of the transition section. The transition sections used in this investigation were standard concentric round to flat oval transitions. Each flat oval test section contained a screen at the inlet to insure a symmetric, flat profile at the inlet of the test section.

The point velocities were taken with a Pitot-static tube connected to a Meriam micromanometer. The Pitot-static tube had an outer diameter of 0.10 inches. The traversing units used were precision units that could indicate position changes of the sensor to within 0.01 inches. Two traversing units were used; one on the major axis, the other on the minor axis. The air temperature was measured in the nozzle section. In addition, the ambient air temperature and the barometric pressure were recorded.

Test Ducts

To determine the flow coefficient independently of the duct aspect ratio, several duct sizes with approximately the same aspect ratio were tested. To determine the influence of aspect ratio on flow coefficient, three different aspect ratios, 2 to 1, 3 to 1, and 4 to 1 were tested. Limitations in available blower capacities prohibited the testing of ducts larger than an equivalent hydraulic round diameter of 12 inches. Each duct was tested at Reynolds' numbers of approximately 0.5×10^5, 1.0×10^5, 1.5×10^5, and 2.0×10^5. A summary of the tests that were run is shown in Table 1. Reynolds' number is calculated using the duct hydraulic diameter (D_H).

TABLE I

A Summary of Tests Run

Nominal Size (in)	Aspect Ratio	Approximate Flow Rate Range (cfm)	Approximate Mean Velocity Range (fpm)	Approximate Reynolds' Number Range ($x10^{-3}$)
3x12	3.97:1	280-1200	1000-4500	50-200
4x15	3.80:1	400-1500	900-4000	50-200
5x19	3.64:1	500-2000	700-3000	50-200
6x25	4.13:1	600-2400	600-2400	50-200
4x12	2.60:1	350-1250	1000-4000	50-200
5x14	2.54:1	400-1600	800-3500	50-200
6x19	3.35:1	500-2000	700-2600	50-200
4x9	2.25:1	250-1000	1000-4500	50-200
5x10	1.88:1	300-1200	900-4000	50-200
6x12	2.11:1	350-1400	800-3400	50-200

The test ducts were constructed of 24 gauge galvanized steel. The 3"x12", 4"x15", 5"x19", 6"x25", and 6"x19" ducts were spiral welded seam duct. The rest were longitudinal welded seam duct. All but the 6"x25" and 6"x19" ducts were supplied in 6' maximum lengths. The 6"x25" and 6"x19" ducts were supplied in 12' maximum lengths. The duct sections were connected, whenever needed, by means of a sleeve connector that slipped over both the duct sections. The 4"x9", 5"x10", and 6"x12" duct sections were connected by the manufacturer with a continuous weld. The concentric round to flat oval transitions were constructed of 20 gauge galvanized steel.

Test Procedure

Since this investigation was done in the entrance region of the ducts, one duct from each aspect ratio group was tested for flow development. Velocity traverses were made at $5D_H$, $10D_H$, and $20D_H$ downstream of the screen. On all other ducts from the same aspect ratio group, traverses were made only at the $10D_H$ station.

Positioning of the Pitot-static Probe

At each traverse station three holes were drilled in the duct. One was drilled on the minor axis and two were drilled on the major axis, as shown in Fig. 3. The holes were smoothed free from burrs so as not to influence the readings near the wall. Two Pitot-static probes with the same diameter were used, each in a separate traversing unit. The traversing units were mounted on platforms which in turn were attached to the duct. Figure 3 illustrates how the platforms were supported. The platforms were supported axially by two sets of 10-32 stove bolts. The platforms were held in place by two adjustable steel bands. To position the unit with respect to the major axis, the traverse unit was fully extended and

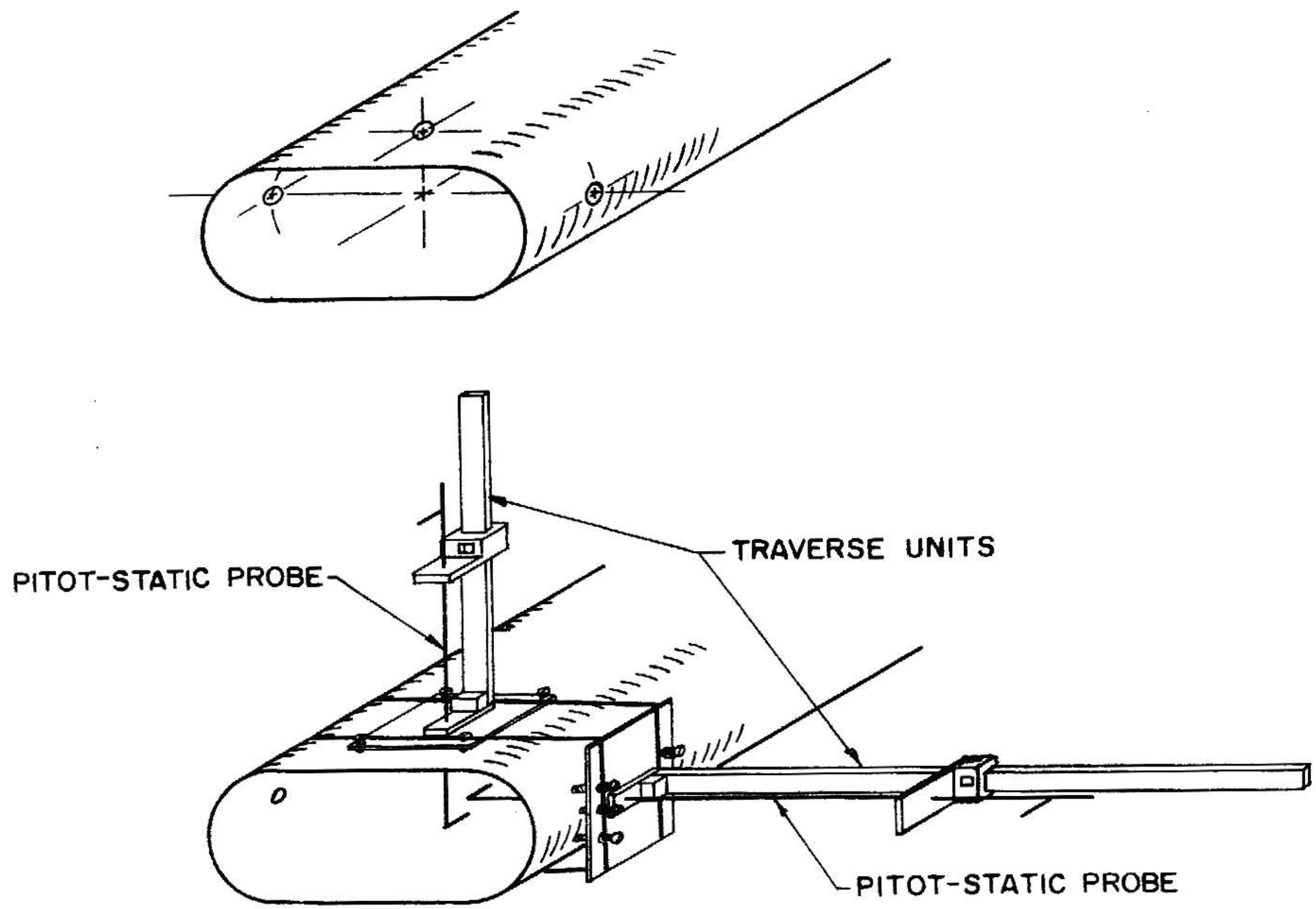

Figure 3. Pitot-static Traverse Mounts.

aligned with the opposite hole on the major axis. The unit on the minor axis was then aligned, by eye, vertical to the major axis unit. The center of the duct was found as the point of intersection of the major axis probe and the minor axis probe. This was checked by using the traverse units' scales to independently find the duct centerline. During the tests, while readings were being taken with one probe, the other probe was positioned near the wall so as not to influence the reading. When the Pitot-static traverse units were moved from one traverse station to the next, the above procedures were repeated.

Startup

Before the initial test on each duct, a check was made to insure that the velocity profile was symmetric to within 5%. All micromanometers were checked for zero and the Pitot-static probes were checked for proper alignment. After the desired flow rate was attained, the apparatus was allowed to run for approximately 1 hour prior to making any measurements.

Test Routine

Each velocity-traverse consisted of velocity-pressure measurements along each axis of the test duct; fluid temperature measurements, nozzle velocity-pressure measurements, and atmospheric-pressure measurements. During the course of each run the nozzle velocity-pressure and fluid temperature were monitored to insure that the system was operating at a steady condition. Data was not taken if the fluid temperature was above 90°F.

CHAPTER III

EXPERIMENTAL RESULTS

Traversing Method

To simplify the calculation of flow rate using the traversing method, it was decided that the Pitot-static probe locations for traversing flat oval duct should be placed in the centers of equal areas. Therefore, in determining the mean velocity, the individual velocities, or the square roots of the velocity-pressure heads may be averaged. To determine the shape and location of the equal areas, Fig. 4, a typical isovel (equal velocity plot) for flat oval ducts was considered. Figure 4 shows equal velocity curves for a 6"x25" flat oval duct at a Reynolds' number of approximately 2.0×10^5. The equal velocity curves resemble the general shape of the duct. Even the center-most ring is of the same shape as the duct boundary, although the aspect ratio of the rings increased as they approached the center of the duct. For most accurate results in predicting the mean velocity, the equal area segments should coincide with the equal velocity rings. With this in mind, it was decided to use equal area rings with flat oval shape and constant aspect ratio equal to the aspect ratio of the test duct. The distances from the centerline of the flat oval duct to the center of the equal area rings on each axis are dependent only on the number of rings and on the length of each respective axis. The complete analysis of the probe locations is given in Appendix C. The positions for 5 and 10 equal area rings are given in Fig. 16 in Appendix C.

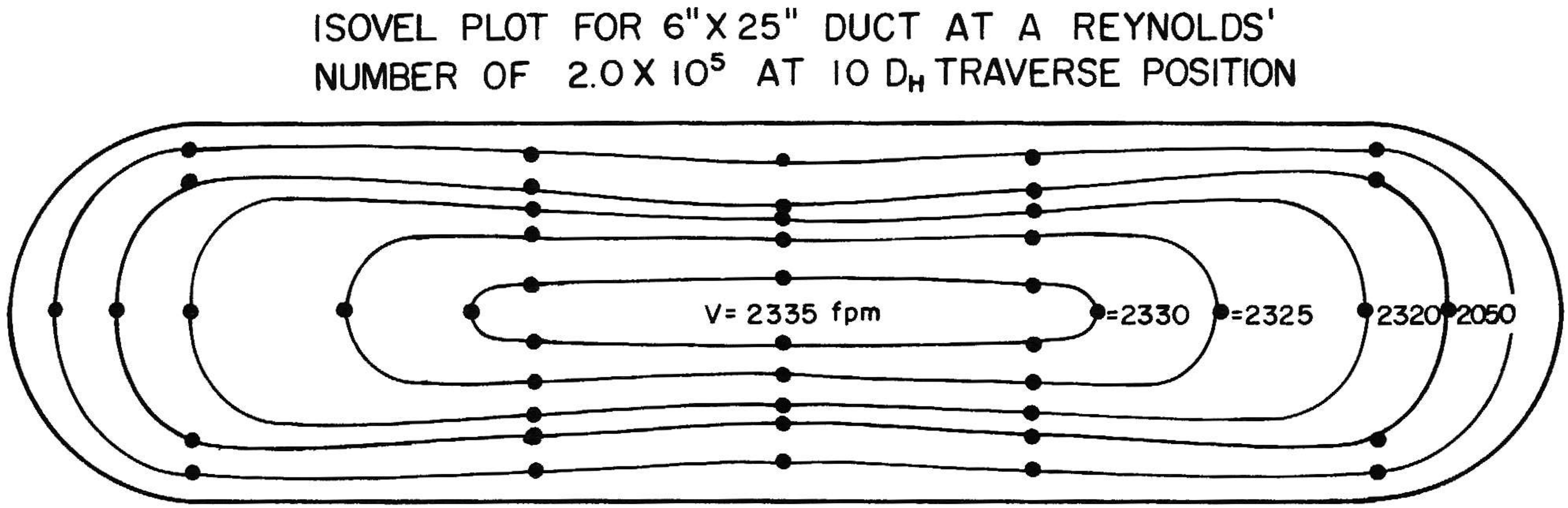

Figure 4. Typical Equal Velocity Plot For Flat Oval Duct In Cross Section.

This method of traversing flat oval ducts is similar to the standard method of traversing circular ducts (3).

In the course of this investigation, traverses were made using both 5 and 10 rings for every test condition.

Table 2 indicates the mean velocities determined by the traversing method described above. Each duct was tested at 4 flow rates. The mean velocities were found by using 10 equal area rings and 5 equal area rings. Each was compared to a mean velocity calculated by dividing the measured volumetric flow rate through the nozzle by the test duct area. Table 2 also indicates the percentage error in the mean velocities predicted by the duct traversing method as compared to the mean velocities calculated using the nozzle flow rate. The extent of agreement between the predicted mean velocities and the mean velocities calculated using the nozzle flow rate is shown in Table 2. The percentage difference columns in Table 2 indicate that the maximum difference was approximately ±4%. The difference in the "mean squares" sense was found to be ±2%. Comparing the percent difference columns for the 10 ring traverse and 5 ring traverse, it can be seen that the 5 ring method predicted the flow rate as well as did the 10 ring method.

Flow Coefficient

The flow coefficient, as used in this investigation, is defined as the duct mean velocity divided by the duct centerline velocity at a point 10 hydraulic diameters downstream of the duct entrance. Table 3 lists the flow coefficients calculated for the tested ducts and the duct Reynolds' number for each test. In each test, flow coefficients were calculated using both the mean velocity from the 10 ring traverse method and the mean velocity calculated from the nozzle flow rate. The difference between these two

TABLE 2

Comparison Between Mean Velocity Prediction
By The Traversing Method and The Mean Velocity
Found From The Known Flow Rate

Duct Nominal Size (in)	Mean Velocity 10 Rings (fpm)	Mean Velocity 5 Rings (fpm)	Mean Velocity Using Nozzle (fpm)	Percent Difference 10 Rings (%)	Percent Difference 5 Rings (%)
3x12	4611	4615	4685	1.6	1.5
3x12	3512	3524	3594	2.3	1.9
3x12	2321	2325	2377	2.3	2.2
3x12	1036	1040	1082	4.2	3.8
4x15	3742	3767	3754	0.3	-0.3
4x15	2802	2815	2825	0.8	0.4
4x15	1867	1867	1869	0.1	0.1
4x15	893	897	912	2.0	1.6
5x19	2882	2874	2861	-0.7	-0.4
5x19	2190	2194	2168	-1.0	-1.2
5x19	1468	1472	1441	-1.9	-2.2
5x19	714	718	713	-0.1	-0.7
6x25	2147	2151	2187	-1.9	-1.7
6x25	1772	1764	1754	-1.0	-0.5
6x25	1267	1267	1260	-0.6	-0.6
6x25	629	629	649	3.0	3.0
4x12	3763	3779	3658	-2.8	-3.3
4x12	2859	2863	2801	-2.1	-2.2

TABLE 2 -- Continued

Duct Nominal Size (in)	Mean Velocity 10 Rings (fpm)	Mean Velocity 5 Rings (fpm)	Mean Velocity Using Nozzle (fpm)	Percent Difference 10 Rings (%)	Percent Difference 5 Rings (%)
4x12	1887	1887	1836	-2.7	-2.7
4x12	1106	1106	1098	-0.8	-0.8
5x14	3917	3922	3810	-2.8	-2.9
5x14	2508	2512	2416	-3.8	-4.0
5x14	1678	1682	1665	-0.7	-1.0
5x14	841	845	820	-2.5	-3.0
6x19	2577	2582	2665	3.3	3.1
6x19	1934	1930	1989	2.8	3.0
6x19	1315	1319	1358	3.2	2.9
6x19	670	678	676	0.8	-0.4
4x9	4489	4484	4480	-0.2	-0.1
4x9	3339	3347	3386	1.4	1.2
4x9	2211	2215	2243	1.5	1.3
4x9	1047	1043	1082	3.2	3.6
5x10	3623	3614	3536	-2.5	-2.2
5x10	2751	2751	2666	-3.2	-3.2
5x10	1838	1838	1782	-3.1	-3.1
5x10	881	885	894	1.5	1.0
6x12	3122	3118	3149	0.8	1.0
6x12	2336	2340	2370	1.4	1.3
6x12	1667	1671	1697	1.8	1.5
6x12	771	771	789	2.3	2.3

TABLE 3

Flow Coefficient and Duct Reynolds' Number

Duct Nominal Size (in)	Mean Velocity 10 Ring (fpm)	Mean Velocity From Nozzle (fpm)	Centerline Velocity (fpm)	Duct Re (x10-5)	Flow Coefficient Using Traverse Mean Velocity	Flow Coefficient Using Mean Velocity From Nozzle
3x12	4611	4685	4802	1.86	0.96	0.98
3x12	3512	3594	3662	1.42	0.96	0.98
3x12	2321	2377	2429	0.95	0.96	0.98
3x12	1036	1082	1103	0.43	0.94	0.98
4x15	3742	3754	3912	1.90	0.96	0.96
4x15	2803	2825	2935	1.44	0.96	0.96
4x15	1867	1869	1958	0.95	0.96	0.96
4x15	893	912	947	0.47	0.94	0.96
5x19	2882	2861	3072	1.89	0.94	0.93
5x19	2190	2168	2343	1.43	0.94	0.93
5x19	1468	1440	1571	0.95	0.93	0.92
5x19	714	713	759	0.47	0.94	0.94
6x25	2147	2188	2340	1.71	0.92	0.94
6x25	1772	1754	1941	1.37	0.91	0.90
6x25	1267	1260	1392	0.97	0.91	0.91
6x25	629	649	691	0.50	0.91	0.94
4x12	3763	3659	3990	1.92	0.94	0.92
4x12	2859	2801	3078	1.47	0.93	0.91

TABLE 3 -- Continued

Duct Nominal Size (in)	Mean Velocity 10 Ring (fpm)	Mean Velocity From Nozzle (fpm)	Centerline Velocity (fpm)	Duct Re ($x10^{-5}$)	Flow Coefficient Using Traverse Mean Velocity	Flow Coefficient Using Mean Velocity From Nozzle
4x12	1887	1836	2043	0.96	0.92	0.90
4x12	1106	1098	1205	0.57	0.92	0.91
5x14	3917	3810	4228	2.40	0.93	0.90
5x14	2508	2416	2732	1.52	0.92	0.88
5x14	1677	1665	1831	1.05	0.92	0.91
5x14	841	820	915	0.52	0.92	0.90
6x19	2577	2665	2768	1.96	0.93	0.96
6x19	1934	1989	2104	1.46	0.92	0.95
6x19	1315	1358	1435	1.00	0.92	0.95
6x19	670	676	732	0.50	0.92	0.92
4x9	4489	4480	4646	1.99	0.97	0.96
4x9	3339	3386	3521	1.51	0.95	0.96
4x9	2211	2243	2339	1.00	0.94	0.96
4x9	1047	1082	1126	0.48	0.93	0.96
5x10	3623	3536	3813	1.89	0.95	0.93
5x10	2751	2666	2896	1.43	0.95	0.92
5x10	1838	1782	1945	0.95	0.95	0.92
5x10	881	894	935	0.48	0.94	0.96
6x12	3122	3149	3284	1.93	0.95	0.96
6x12	2336	2370	2884	1.46	0.94	0.95
6x12	1667	1697	1778	1.05	0.94	0.95
6x12	771	789	825	0.49	0.93	0.96

flow coefficients is, in effect, the difference between the two mean velocities used. The flow coefficients were, for the most part, above 0.90 and below 0.96. In each duct the flow coefficient decreased slightly with decreasing Reynolds' number. There was no apparent difference in flow coefficients for different aspect ratios. Figures 5, 6, and 7 show flow coefficients calculated using the 10-ring traverse method, as a function of Reynolds' number for aspect ratios of 4:1, 3:1, and 2:1 respectively. In Fig. 5, for the 4:1 aspect ratio, the slight scattering of the data points is attributed to the local irregularities of the smaller test ducts, i.e. in the smaller test ducts the maximum velocity was not located on the centerline. The smaller test ducts were somewhat "caved in" along the flat span. That is the duct height on the minor axis was less at the center of the duct than on either side of the centerline. This caused the maximum velocity to be located, not on the duct centerline, but at points on either side of the minor axis where the duct height was a maximum (see Fig. 14). This irregularity tended to increase the flow coefficient because the centerline velocity was not the maximum velocity. The larger the test duct, the smaller was the effect of this irregularity.

Figure 8 is a plot of all of the flow coefficients versus Reynolds' number regardless of duct aspect ratio. The line through the experimental points is a "least squares" fit of the data having a 95% confidence interval of $\pm 2\%$. The line extends from C_F=0.929 at Re=0.5×10^5 to C_F=0.945 at Re=2.40×10^5. The flow coefficients decreased slightly with decreasing Reynolds' number. This trend was expected after noting that flow coefficients for fully developed flow in smooth circular ducts decrease almost linearly with Reynolds' number in the same Reynolds' number range (4).

Figure 8, plus an iteration technique, can be used to determine the mean velocity in flat oval ducts by measuring only the centerline velocity. Using the measured value of centerline velocity and assuming the initial flow coefficient

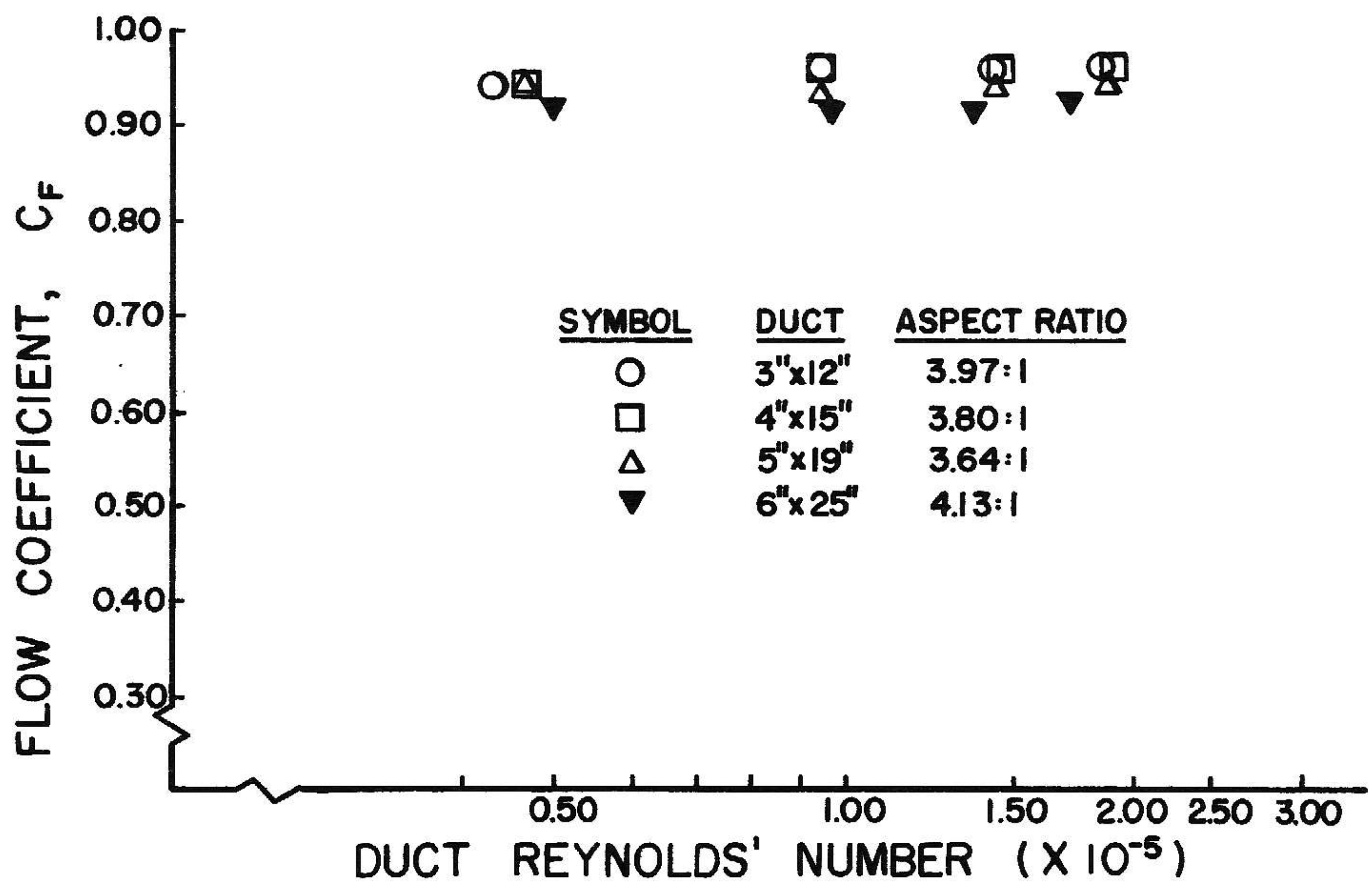

Figure 5. Flow Coefficient Versus Reynolds' Number for Aspect Ratio of 4:1.

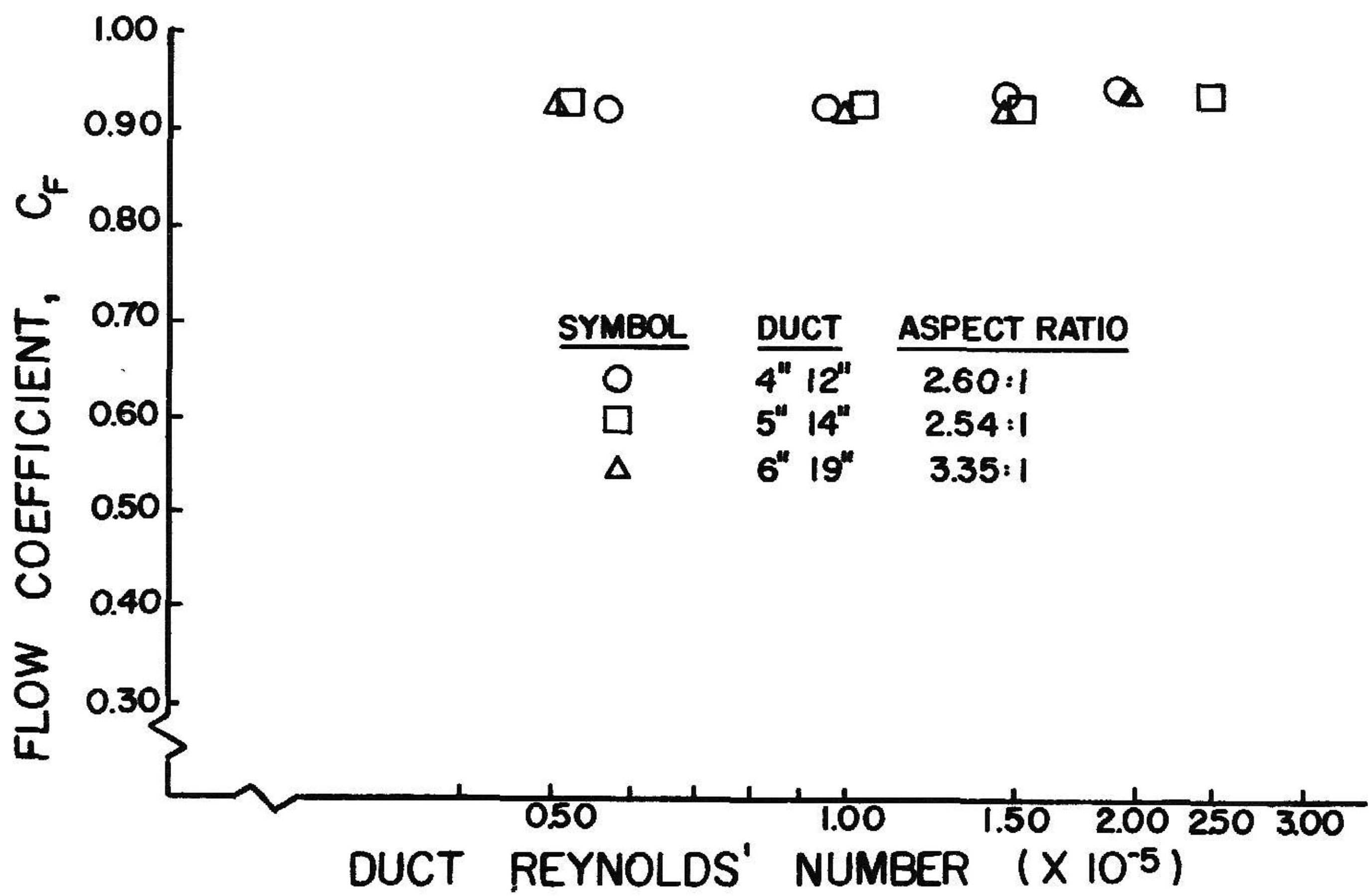

Figure 6. Flow Coefficient Versus Reynolds' Number for Aspect Ratio of 3:1.

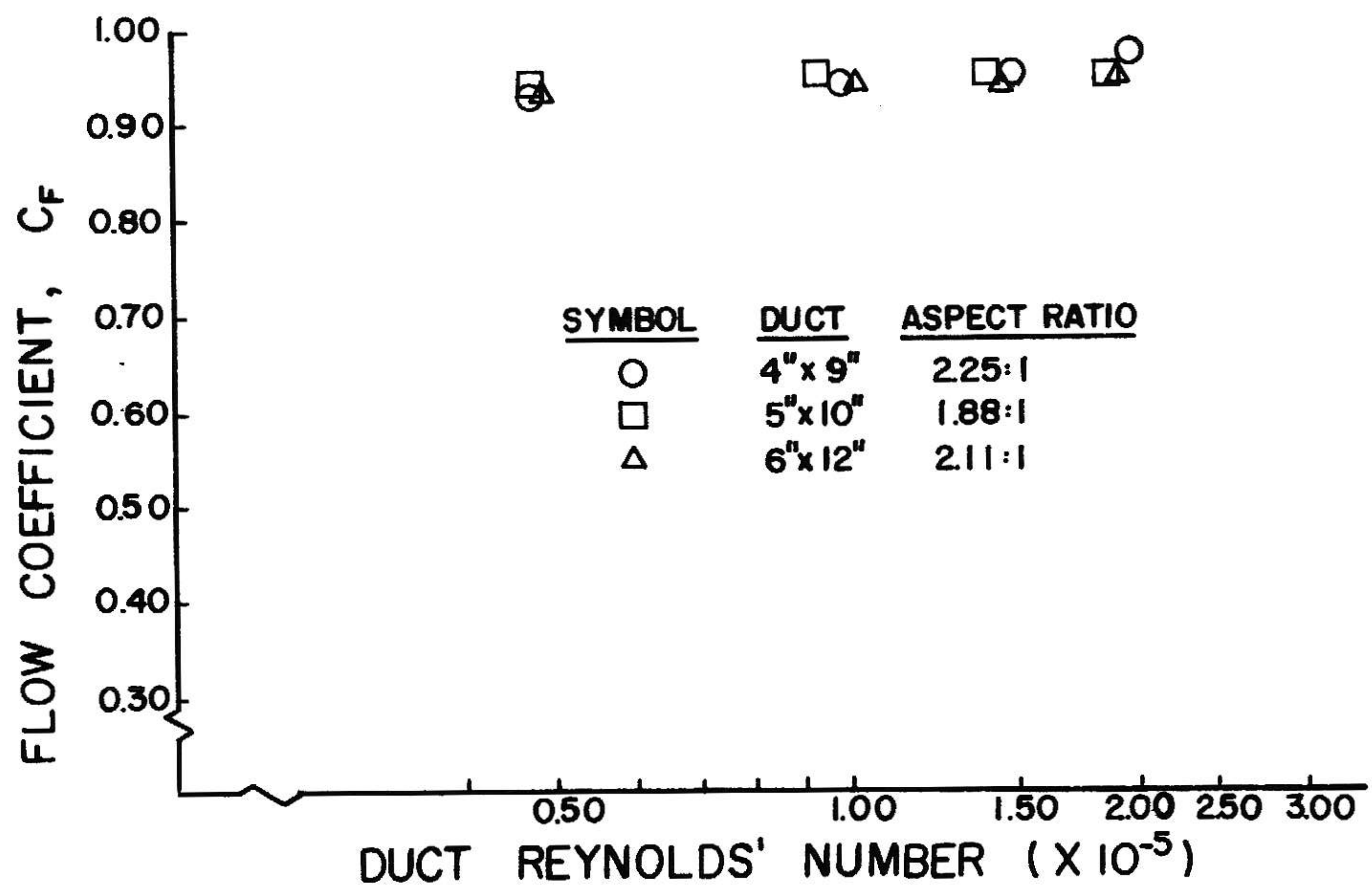

Figure 7. Flow Coefficient Versus Reynolds' Number for Aspect Ratio of 2:1.

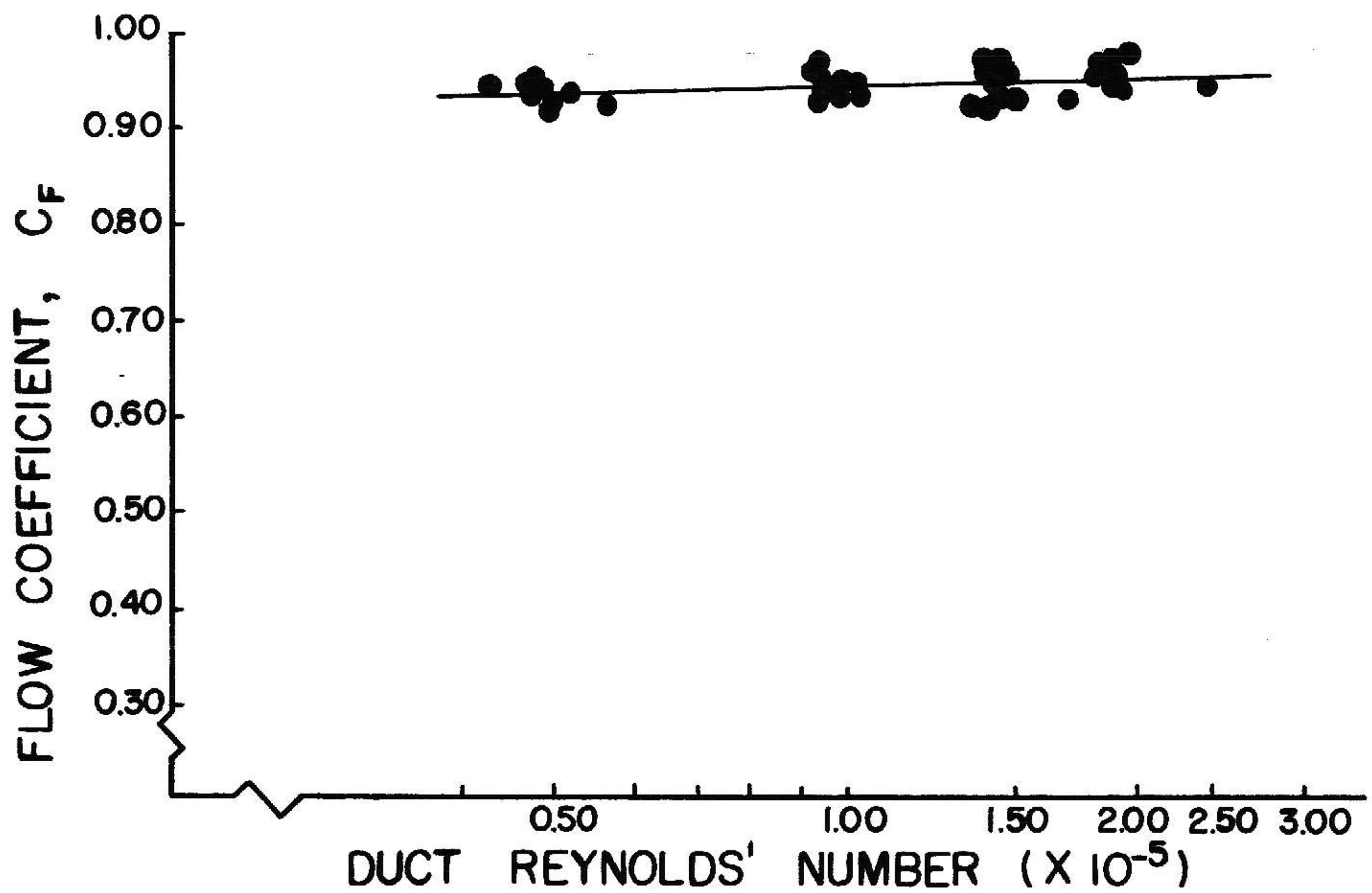

Figure 8. Flow Coefficient Versus Reynolds' Number for All Aspect Ratios Tested.

to be 1.00, an initial Reynolds' number can be calculated from equation (3-1).

$$Re = (C_F V_{\mathbb{C}} D_H)/\nu \qquad (3\text{-}1)$$

Using this Reynolds' number, a value for flow coefficient can be obtained from Fig. 8. From this new value of flow coefficient a new Reynolds' number can be calculated using equation (3-1). This procedure is continued until successive flow coefficients obtained from Fig. 8 are the same.

Variation of Flow Coefficient Within Entrance Region

Since this investigation was done in the entrance region of the duct, traverses were made on selected ducts at points 5 D_H, 10D_H, and 20D_H downstream of the entrance. This was done to investigate the variation of flow coefficient within the entrance region. Test ducts selected for this study included the smallest duct in each aspect ratio group. The tests were taken only at the highest Reynolds' number because it was expected that the longest entrance length would give the largest error in flow coefficient between points downstream. The longest entrance length is associated with the largest Reynolds' number.

Figure 9 illustrates the velocity profiles along the minor axis for the 3"x12" duct ($AR \approx 4:1$) at a Reynolds' number of 1.86×10^5. The profiles are plotted as point velocities divided by the centerline velocity on the abscissa and distance from duct centerline divided by one half the minor axis on the ordinate. Figure 10 shows the velocity profiles on the major axis for the 3"x12" duct. Figures 11 and 12 illustrate the velocity profiles for the 4"x12" duct ($AR \approx 3:1$) at a Reynolds' number of 1.92×10^5 and Fig. 13 and Fig. 14 illustrate the profiles for the 4"x9" duct ($AR \approx 2:1$) at a Reynolds' number of 1.99×10^5. The major axis profiles show the tendency of the maximum velocity to be somewhat shifted from the centerline. This irregularity was discussed earlier and was caused by the

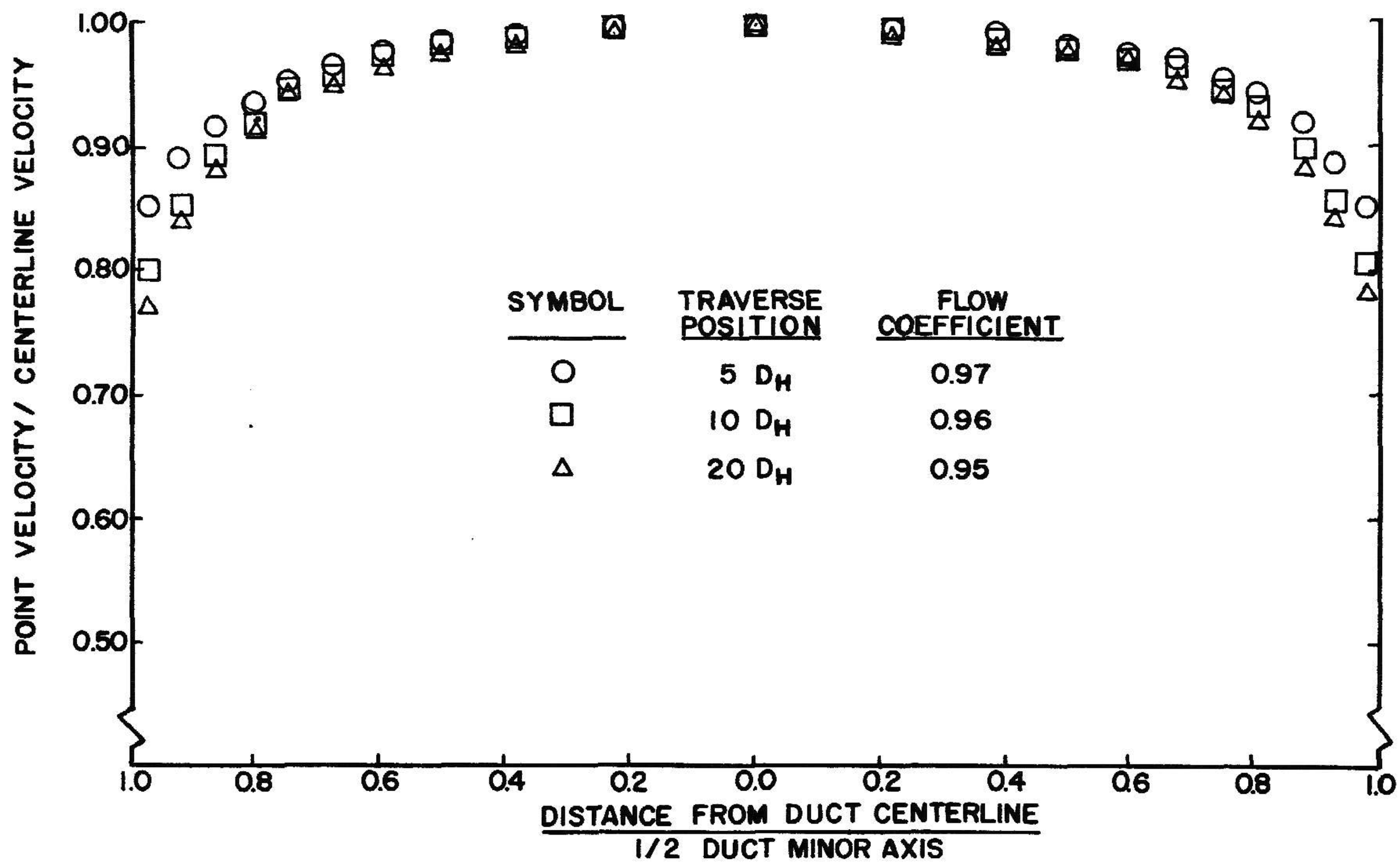

Figure 9. Velocity Profiles Along Minor Axis at $5D_H$, $10D_H$, and $20D_H$, Downstream of the Entrance for 3"x12" Duct at a Reynolds' Number of 1.86×10^5.

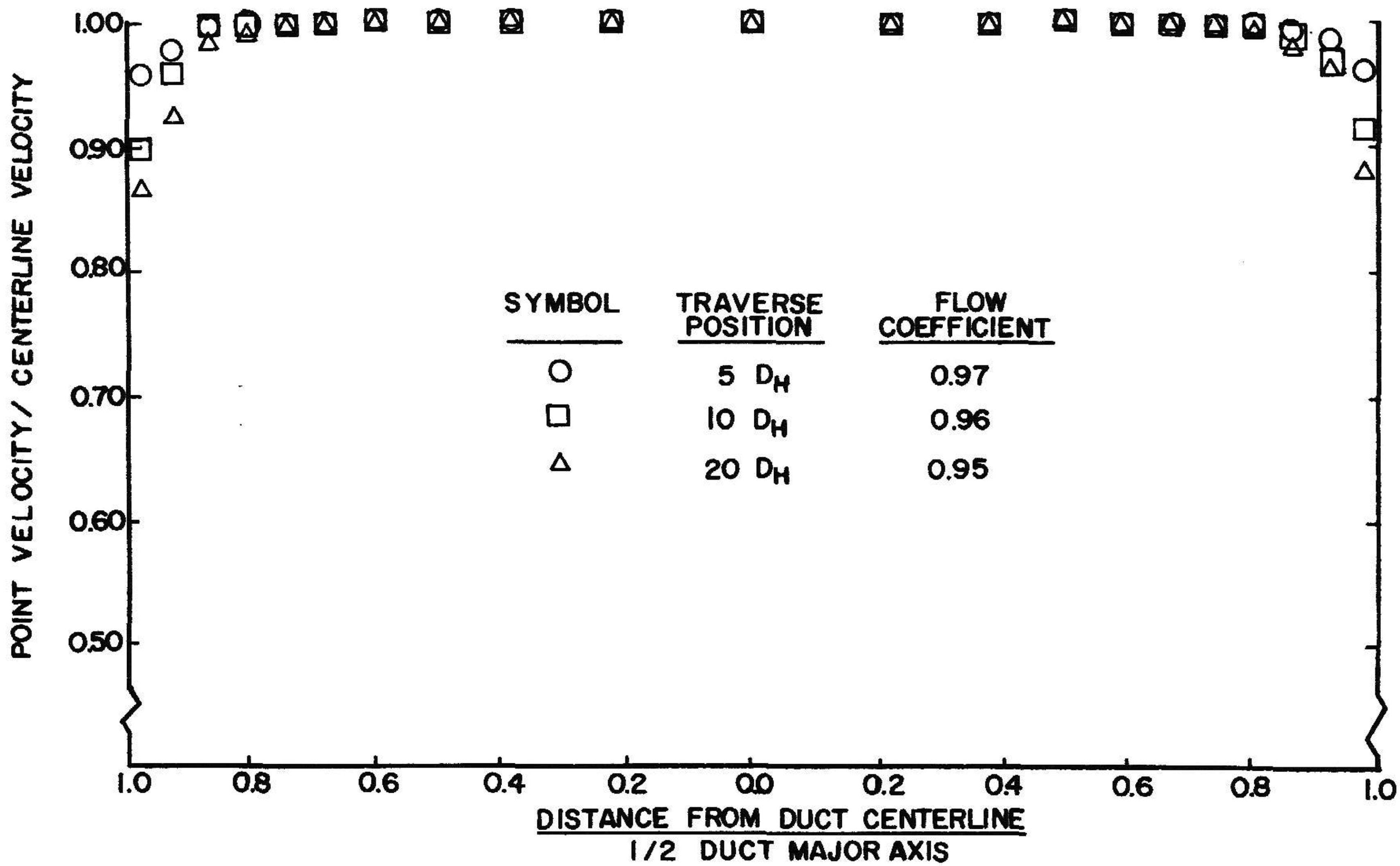

Figure 10. Velocity Profiles Along Major Axis at $5D_H$, $10D_H$, And $20D_H$ Downstream of the Entrance for 3"x12" Duct at a Reynolds' Number of $1.86x10^5$.

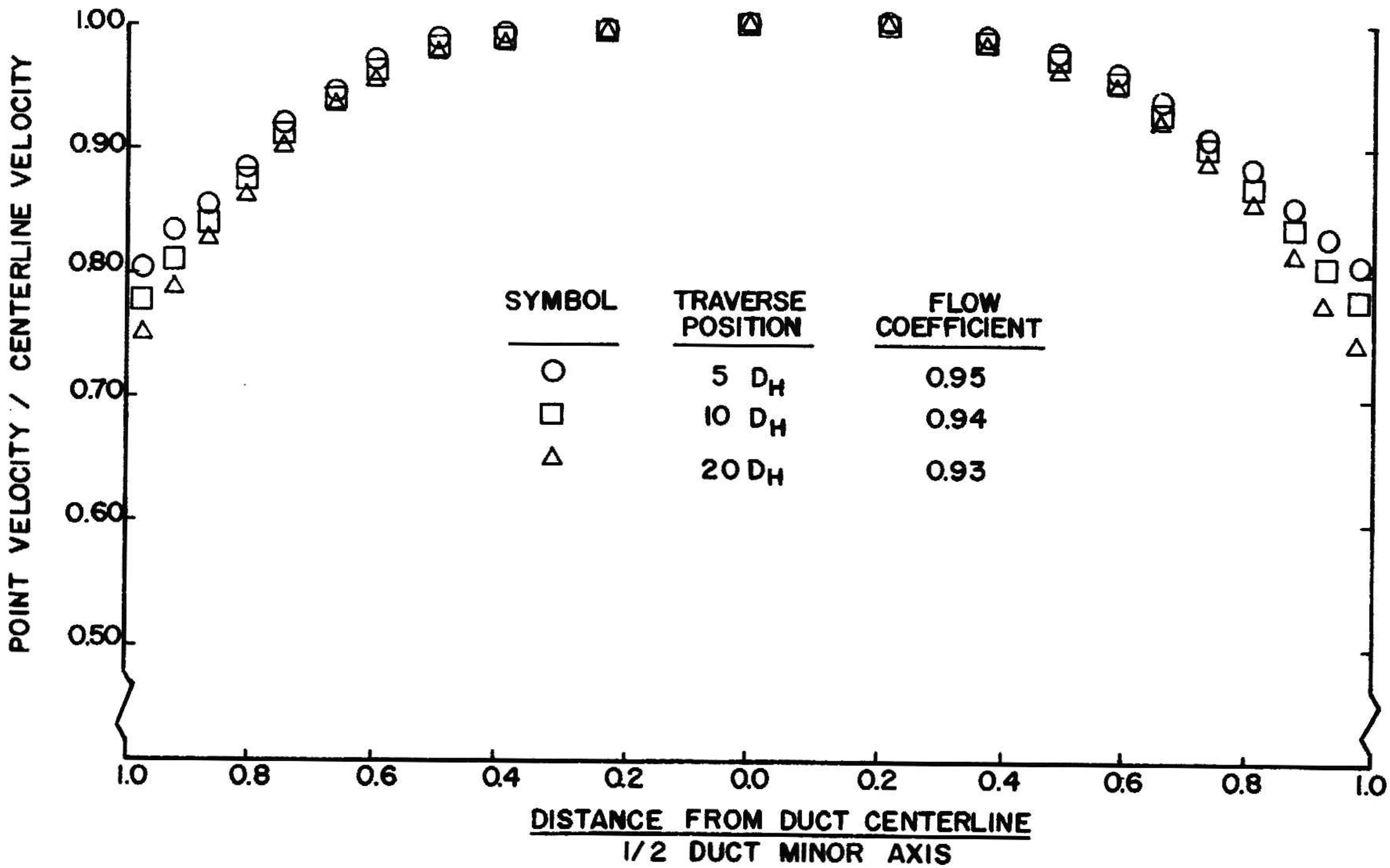

Figure 11. Velocity Profiles Along Minor Axis At $5D_H$, $10D_H$, And $20D_H$ Downstream of the Entrance for 4"x12" Duct at a Reynolds' Number of $1.92x10^5$.

ILLEGIBLE DOCUMENT

THE FOLLOWING DOCUMENT(S) IS OF POOR LEGIBILITY IN THE ORIGINAL

THIS IS THE BEST COPY AVAILABLE

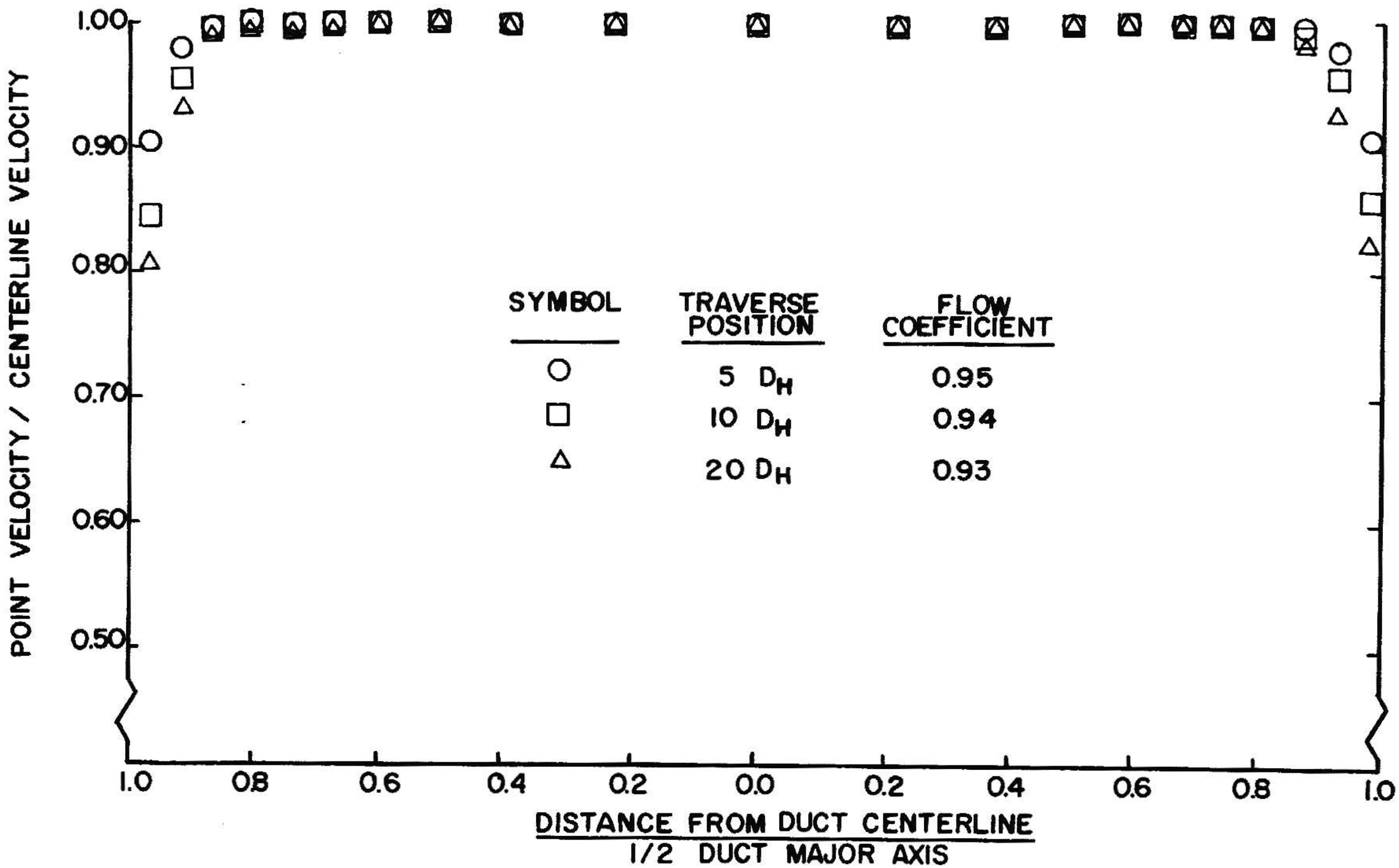

Figure 12. Velocity Profiles Along Major Axis At $5D_H$, $10D_H$, And $20D_H$, Downstream of the Entrance for 4"x12" Duct at a Reynolds' Number of 1.92×10^5.

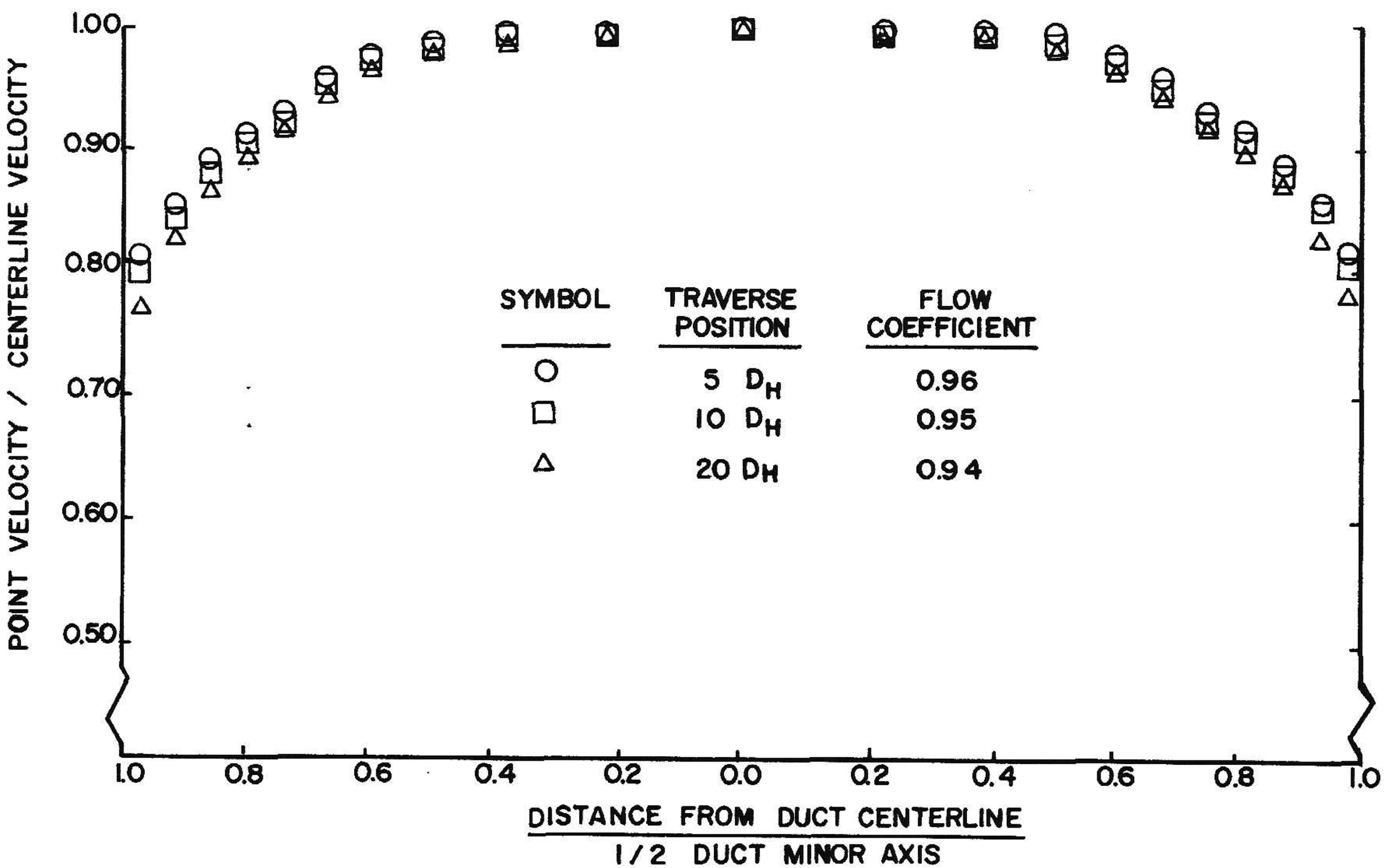

Figure 13. Velocity Profiles Along Minor Axis at $5D_H$, $10D_H$, And $20D_H$ Downstream of the Entrance for 4"x9" Duct at a Reynolds' Number of 1.99×10^5.

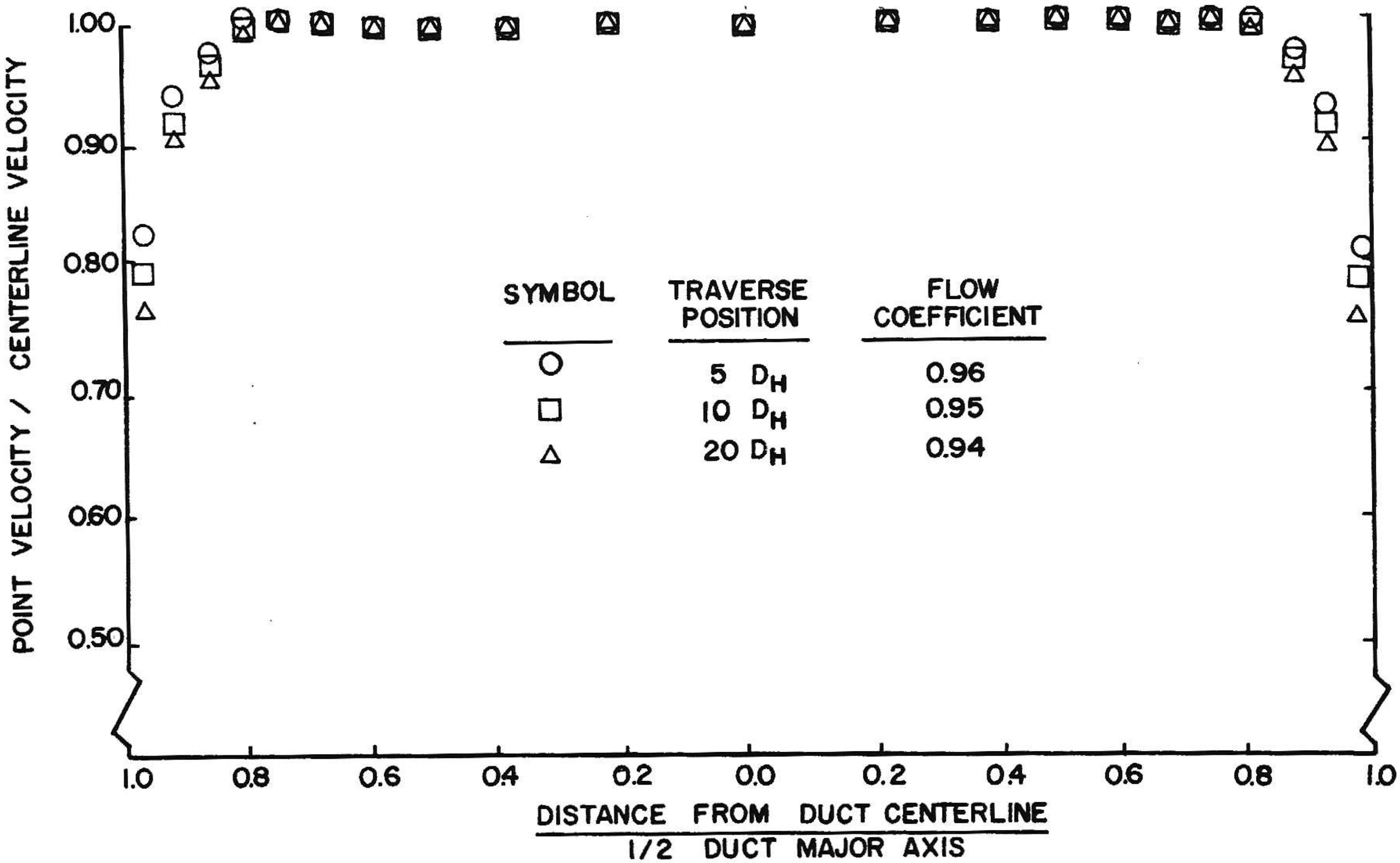

Figure 14. Velocity Profiles Along Major Axis At $5D_H$, $10D_H$, And $20D_H$ Downstream of the Entrance for 4"x9" Duct at a Reynolds' Number of 1.99×10^5.

tendency of the smaller ducts to be somewhat "caved in" on the flat span. The minor axis velocity profiles are more "parabolic" than the velocity profiles along the major axis. This would indicate that the minor axis velocity profile is more fully developed at each plane than is the major axis velocity profile. However, it should be noted that the velocity profiles on both the major and minor axes become more "parabolic" as the distance downstream of the entrance is increased. The centerline velocity increases and therefore the flow coefficient decreases downstream.

For each duct, the flow coefficients changed by only 1% from one traverse station to the next. This indicates that flow coefficients are affected somewhat by the measuring location, but the values taken at any point between 5 D_H and 20 D_H will be at least within 1% of the values at 10 D_H.

Error Discussion

The purpose of this section is to discuss the possible errors which may have affected the results described above. These errors include fluctuations in the power to the d.c. fan motor, irregularities in the duct shape, errors in placement of the Pitot-static probe, and velocity measurement errors.

Although the amount of power to the d.c. motor was closely attended, some fluctuations in the line voltage supplied to the experimental area were noticed. When these fluctuations were noted, data taking ceased until the line voltage had resumed its normal value. If the voltage change was prolonged the d.c. motor rheostat was adjusted accordingly. The maximum instantaneous error in air flow rate was estimated to be $\pm 2\%$. It should be pointed out however, that these fluctuations, when they did occur, were usually of short duration, and the cumulative error in flow rate for each test was probably much less than the ±2% instantaneous difference.

Irregularities in the test duct shape were noted earlier in this report. The smaller test ducts were observed to be somewhat "caved in" along the flat span. The maximum point of deflection was at the center of the duct. This irregularity tended to shift the maximum velocity from the centerline to a point along the major axis to either side of the centerline. This shifting of the maximum velocity point, in effect, lowered the centerline velocity, thus increasing the calculated flow coefficient. An exact value of the error due to the duct irregularity would be difficult to determine.

Differences in the test duct construction also caused errors in determining the exact duct area. This is always a problem in measurement of flow rates in ducts. The inside duct dimensions can be measured to some desired degree of accuracy at the duct exit but there is no assurance that these dimensions are exactly the same at the duct measurement plane. Comparing mean velocities obtained by the duct traverse method to the mean velocities calculated by dividing the nozzle volumetric flow rate by the test duct area, it was noted that the two methods agreed to within a maximum error of ±4% and a mean square error of ±2%. Since the traverse method obtains a mean velocity independent of the duct area, and the volumetric flow rate is known to a high degree of accuracy (±1%), the small difference between the two methods is a good indication that there was little error in measuring the test duct areas.

Errors in placement of the Pitot-static probe and velocity measurement errors were estimated to be minimal. Since the velocity profiles were quite flat at the 10 D_H measuring station, a relatively large error in placing the Pitot-static probe would cause a very small error in the velocity reading. The velocity-pressure readings were taken with a micromanometer capable of accuracy of ±0.002 inches H_2O (3). The Pitot-static probes used were capable of a precision from ±1% to ±4% (3), with the ±4% estimate being applied at the low end of the velocity range considered in this investigation.

CHAPTER IV

CONCLUSIONS AND RECOMMENDATIONS

It is concluded from these experimental results that an accurate and efficient means of determining air flow rates in flat oval ducts has been developed. This investigation proposed and substantiated two methods by which air flow rates can be measured in flat oval ducts.

The first was to apply a traversing method to obtain a mean velocity within the duct. Using this mean velocity, the volumetric flow rate can be obtained to approximately the degree of accuracy to which the duct area is known. This method can be used when the volumetric flow rate must be known to the highest degree of accuracy.

When the flow rate need not be known to the highest degree of accuracy, a second method of flow measurement may be employed. This second method consists of measuring a single velocity at the duct centerline and multiplying this centerline velocity by the appropriate flow coefficient and duct area to obtain the flow rate. This flow rate, since it is dependent upon only one measurement, is affected to a greater extent by the local irregularities of the duct than is the flow rate calculated by the traversing method. This flow coefficient was also found to be a function of the flow development, therefore care should be taken to account for entrance effects when using this method.

For future investigation, it would be desirable to test a wider range of duct aspect ratios and Reynolds' numbers. A recommendation is also made to be assured that each test duct is uniform in shape so that the duct area may be determined to a high degree of accuracy and so that the local irregularities will be minimal.

REFERENCES

1. "Flat Oval Duct and Fittings," United Sheet Metal Co., Inc., Bulletin FO. #7.

2. "Flat Oval Duct Reinforcement and Assembly," United Sheet Metal Co., Inc., Bulletin FO. #8.

3. American Society of Heating, Refrigerating and Air Conditioning Engineers' "Handbook of Fundamentals," ASHRAE, 1967.

4. Knudsen and Katz, Fluid Dynamics and Heat Transfer, New York, McGraw Hill, 1958.

5. ASME Power Test Code; Chapter 4, "Flow Measurement," PTC 19.5; 4-1959.

6. Olsen, Reuben M., Engineering Fluid Mechanics, Scranton, Penn., International Textbook Co., 1968.

7. Schenck, Hilbert, Jr., Theories of Engineering Experimentation, New York, McGraw Hill, 1968.

8. Berry, C. Harold, Flow and Fan, Principles of Moving Air Through Ducts, New York, Industrial Press, 1954.

9. Schlichting, H., Boundary Layer Theory, New York, McGraw Hill, 1955.

10. S. Ahmed and J. Brundrett, "Turbulent Flow In Non-Circular Ducts. Part I. Mean flow properties in the developing region of a square duct," International Journal of Heat and Mass Transfer, Vol. 14, No. 3, March 1971.

11. S. T. McComas, "Hydrodynamic Entrance Lengths for Ducts of Arbitrary Cross Section," Trans. ASME, Vol. 89, 1967, p. 847.

APPENDIX

APPENDIX A

SUPPORT EQUIPMENT LIST

The following is a list of the support equipment and instruments which were required for this investigation.

1. Micromanometer, 10" H_2O range, Meriam Co., serial no. L75571, ME 1280.
2. Micromanometer, 10" H_2O range, Meriam Co., serial no. G10571, ME 1342.
3. 18" Traverse Unit, United Sensor and Control Corp., part no. USC-1108-18, ME 1717.
4. 18" Traverse Unit, United Sensor and Control Corp., part no. USC-1108-18, ME 3713.
5. Pitot-static probe, United Sensor and Control Corp., part no. PAC-18-KL.
6. Pitot-static probe, United Sensor and Control Corp., part no. PAC-24-KL.

APPENDIX B

TABLE 4

Typical Data - Test of Flat Oval Duct 6"x25" 10 Rings

Re = 200,000 Date 5-22-71

6" Nozzle Nozzle Velocity Pressure Head 5.341 in. H_2O
Fluid temp. 81.0°F Atmospheric Pressure 29.01 in. Hg

Distance From Centerline on Minor Axis	Velocity-Pressure-Head (in. H_2O) h upper	h lower
0.0	0.324	0.324
0.224R=0.67	0.316	0.317
0.387R=1.16	0.309	0.309
0.500R=1.50	0.303	0.300
0.592R=1.78	0.290	0.285
0.671R=2.01	0.280	0.275
0.742R=2.23	0.260	0.257
0.806R=2.42	0.243	0.240
0.886R=2.60	0.221	0.224
0.922R=2.77	0.197	0.195
0.975R=2.93	0.147	0.157

Distance From Centerline on Major Axis	Velocity-Pressure-Head (in. H_2O) h north	h south
0.0	0.324	0.324
0.224L=2.22	0.324	0.322
0.387L=3.98	0.323	0.321
0.500L=5.02	0.317	0.318
0.592L=5.94	0.312	0.310
0.671L=6.72	0.311	0.309
0.742L=7.45	0.308	0.304
0.806L=8.10	0.298	0.297
0.886L=8.70	0.288	0.290
0.992L=9.26	0.268	0.264
0.975L=9.79	0.199	0.201

APPENDIX C

DETERMINATION OF THE PITOT-STATIC PROBE LOCATIONS FOR TRAVERSE

The Pitot-static probe locations are the centers of equal area rings. The center of an equal area ring is such that the same area is on either side of the center. Therefore, the duct is divided into twice as many rings as desired. The centers of the equal area rings are the boundaries of the 1,3,5,...2n-1 (n = 1,2,3,...k) rings, where k is the total number of centers of areas. Using Fig. 15 note that the area of the first ring from the center, A_1, is given by:

$$A_1 = \pi D_1^2/4 + (L_1 - D_1)\, D_1$$

and noting that:

$$L_1/D_1 = L/D = AR \text{ (aspect ratio of the duct)}$$

and $A_1 = A_T/2k$ where k = number of centers of rings.

then:

$$A_T/2k = D_1^2\,(AR - 1.0 + \pi/4) \quad \text{or} \quad D_1 = \sqrt{\frac{A_T}{(AR - 1. + \pi/4)\, 2k}}$$

similarly:

$$D_2 = \sqrt{\frac{3A_T}{(AR - 1.0 + \pi/4)\, 2k}}$$

and the n^{th} center of area is given by:

$$D_n = \sqrt{\frac{(2n-1)\, A_T}{(AR - 1.0 + \pi/4)\, 2k}}$$

k = number of centers of rings
(n = 1,2,3,...k)

note that:

$$D = \sqrt{\frac{A_T}{(AR - 1.0 + \pi/4)}} \quad \text{and } R = D/2$$

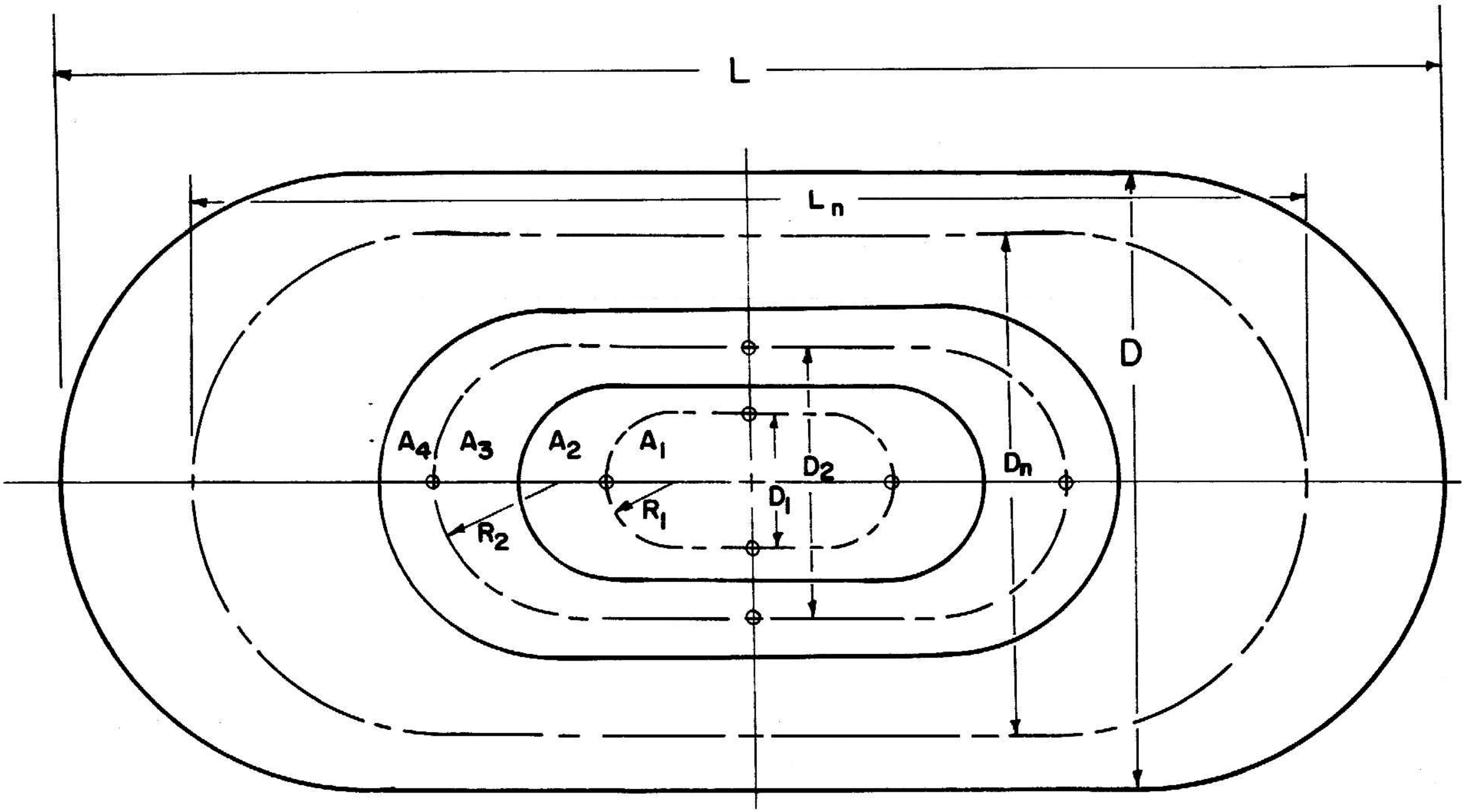

Figure 15. Determination of Pitot-static Probe Locations.

therefore:

$$D_n = \sqrt{\frac{(2n-1)}{2k}} \cdot D \qquad \text{and } R_n = \sqrt{\frac{(2n-1)}{2k}} \cdot R$$

and using a similar analysis:

$$L_n = \sqrt{\frac{(2n-1)}{2k}} \cdot L$$

Figure 16 illustrates the Pitot-static probe locations for 5 equal area rings and for 10 equal area rings.

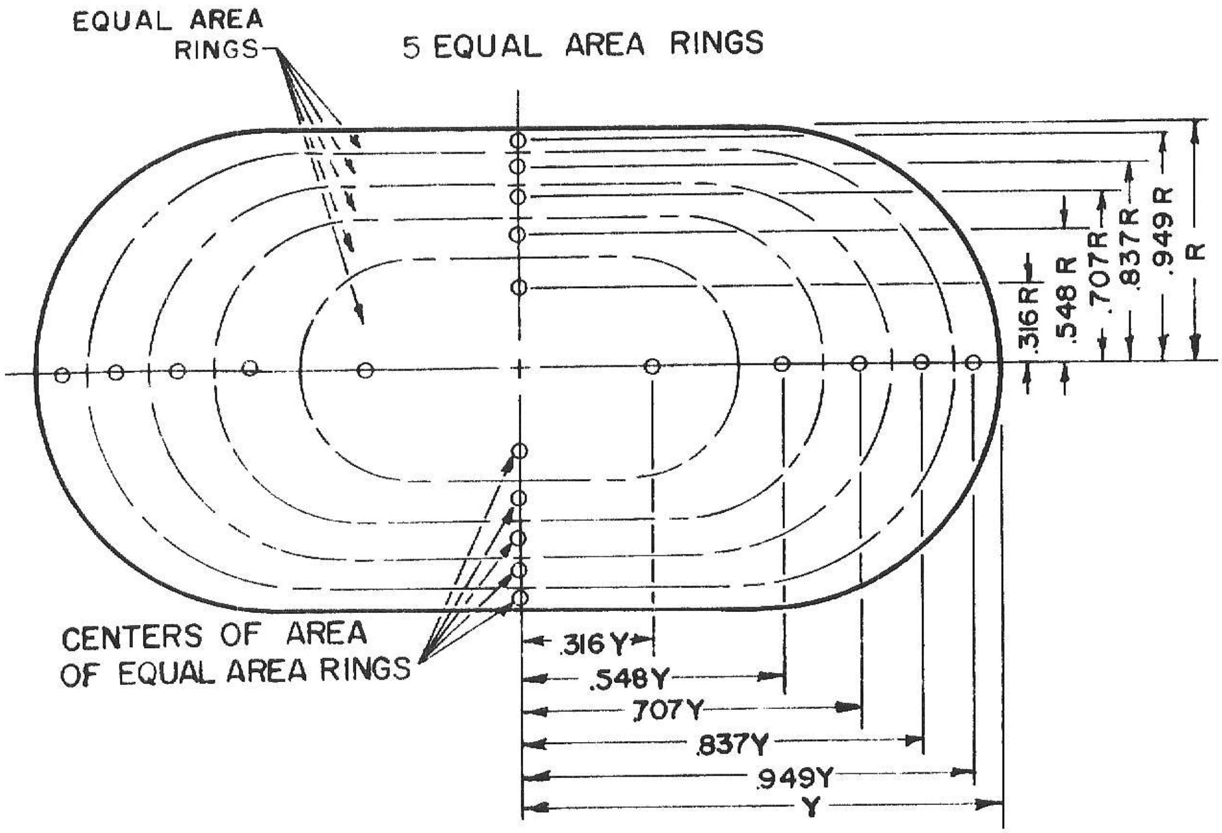

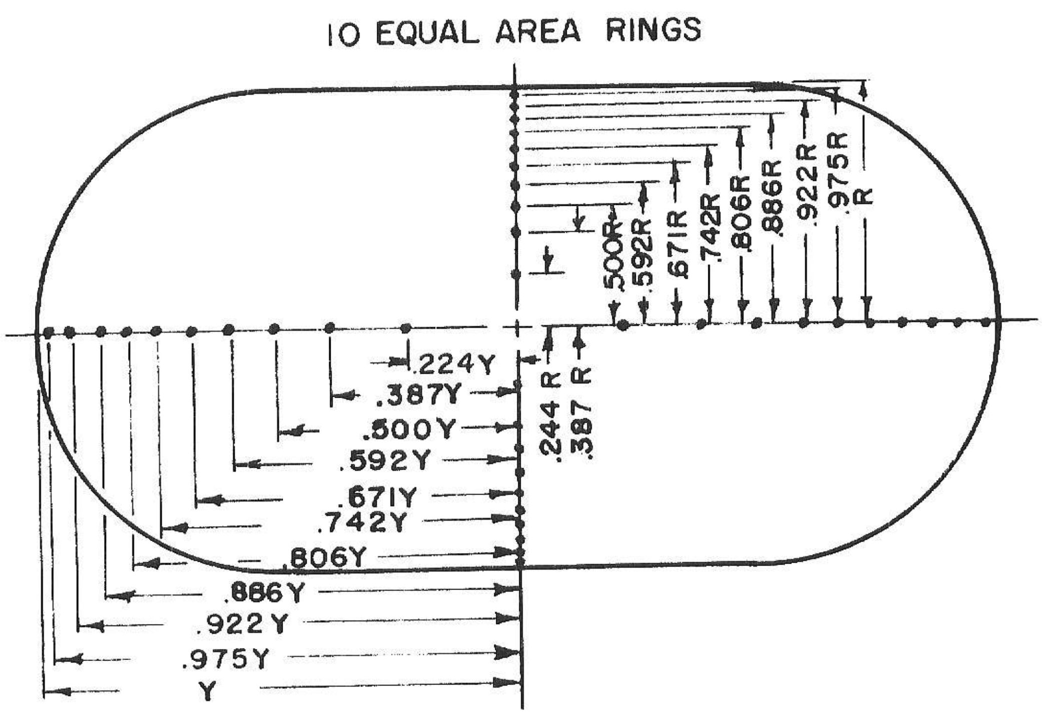

Figure 16. Pitot-static Probe Locations for 5 Equal Area Rings And 10 Equal Area Rings.

VITA

Terrence D. Mayhill

Candidate for the Degree of

Master of Science

Thesis: A SIMPLIFIED METHOD FOR THE MEASUREMENT OF AIR FLOW RATES IN FLAT OVAL DUCTS

Major Field: Mechanical Engineering

Biographical:

Personal Data: Born at Minneapolis, Minnesota, September 4, 1948, the son of Max M. and Leona E. Mayhill.

Education: Graduated from Newton High School, Newton, Kansas, in 1966; attended Bethel College, North Newton, Kansas from September, 1966 to June, 1967; attended Kansas State University, Manhattan, Kansas from September, 1967 to July, 1971; received a Bachelor of Science degree in Mechanical Engineering from Kansas State University in June 1970; completed requirements for Master of Science degree in Mechanical Engineering in July, 1971.

Professional Experience: Was employed as an undergraduate research assistant by the Mechanical Engineering Department at Kansas State University, Manhattan, Kansas from June, 1969 to August, 1970; was a National Science Foundation Trainee at Kansas State University, Manhattan, Kansas from September, 1970 to August, 1971.

A SIMPLIFIED METHOD FOR MEASUREMENT OF AIR FLOW RATES IN FLAT OVAL DUCTS

by

TERRENCE D. MAYHILL

B. S., Kansas State University, 1970

AN ABSTRACT OF A THESIS

submitted in partial fulfillment of the

requirements for the degree

MASTER OF SCIENCE

Department of Mechanical Engineering

KANSAS STATE UNIVERSITY
Manhattan, Kansas

1971

Name: Terrence D. Mayhill　　　　　　　　Date of Degree: 1971

Institution: Kansas State University　　　　　Location: Manhattan, Kansas

Title of Study: A SIMPLIFIED METHOD FOR THE MEASUREMENT OF AIR FLOW RATES IN FLAT OVAL DUCTS

Pages in Study: 42　　　　　Candidate for Degree of Master of Science

Major Field: Mechanical Engineering

Scope and Method of Study: In recent years the air handling industry has begun using a flat oval shaped duct designed for low headroom spaces and restricted ceiling plenum spaces. Since these ducts are relatively new to the air handling industry, test data is somewhat scarce. At the present time there is no proven, practical method for the measurement of volumetric air flow rates in flat oval ducts. The ideal situation would be to measure only one velocity, the centerline velocity, and multiply this velocity by a single known flow coefficient and the duct area to obtain the desired air flow rate. This coefficient would be calculated experimentally by the mean duct velocity divided by the centerline velocity. Or for more accurate results, use a proven method of traversing the flat oval duct to obtain a mean velocity. Multiply this mean velocity by the duct area to obtain the desired air flow rate. The purpose of this study was to develop a method of traversing flat oval ducts and to develop a correlation between flow coefficient and some dimensionless parameter, such as Reynolds' number.

To accomplish the desired objective, an experimental program was undertaken. Test ducts ranged in aspect ratio from 2:1 to 4:1. The ducts were tested at Reynolds' numbers of approximately 0.5×10^5, 1.0×10^5, 1.5×10^5 and 2.0×10^5.

Findings and Conclusions: For ease of mean duct velocity calculations, the centers of equal area rings were used for traverse velocity probe

stations. After considering a typical isovel plot for a flat oval duct, it was decided to use equal area rings with flat oval shapes and constant aspect ratio equal to the aspect ratio of the test ducts. Using this method it was observed that the volumetric flow rate can be calculated to approximately the degree of accuracy to which the duct area is known. When the measuring method is to be simple but the mean velocity need not be known to a high degree of accuracy, the second method of flow measurement may be employed. This second method consists of measuring a single velocity at the duct centerline and multiplying this centerline velocity by the appropriate flow coefficient to obtain a mean velocity. The flow coefficient was found to range from 0.90 to 0.96 depending upon the duct Reynolds' number. The flow coefficient was observed to be a function of the state of flow development and local irregularities in the duct.

MAJOR PROFESSOR'S APPROVAL ____________________________